Single-crystal barium titanate thin films by ion slicing

T. Izuhara,[a] I.-L. Gheorma, and R. M. Osgood, Jr.[b]
Microelectronics Sciences Laboratories, Columbia University, New York, New York 10027

A. N. Roy and H. Bakhru
Department of Physics, State University of New York at Albany, Albany, New York 12222

Yiheli M. Tesfu and M. E. Reeves
Department of Physics, George Washington University, Washington, D.C. 20052

(Received 19 September 2002; accepted 3 December 2002)

Thin barium titanate films, 0.5–8 μm thick, are obtained from a single-crystal bulk sample using ion slicing. The process, based on ion implantation and anodic bonding, separates thin films having areas of $\sim 1\times 1$ cm^2, from bulk crystals. The quality of the film is characterized by measurement of surface roughness and dielectric properties. The film permittivity retains its single-crystal value. © *2003 American Institute of Physics.* [DOI: 10.1063/1.1540727]

Barium titanate, $BaTiO_3$ (BTO), is a ferroelectric crystal whose outstanding electrical and optical properties make it an important material for numerous applications.[1–4] These include, for example, a very high dielectric constant for capacitors, a large pyroelectric coefficient for pyroelectric detectors, and large nonlinear coefficients for applications in nonlinear optics. Many of these applications require a thin-film form rather than a bulk crystal. While significant advances have occurred in deposition of thin BTO films,[5] these films still do not possess the properties of bulk BTO, that is high-quality, single-crystal thin-films are difficult if not impossible to obtain, and require lattice matching to the growth substrate. Recently, a new method of obtaining single-crystal thin-films has been developed and demonstrated for such materials as $LiNbO_3$, $LiTaO_3$, $SrTiO_3$, $KTaO_3$, and YIG.[6–9] This method, which we have called crystal ion slicing (CIS), can slice a 0.5–10-μm-thick layer of material from a bulk single-crystal wafer by implanting the wafer with high-energy ions and subsequent thermal treatment or wet etching of the buried sacrificial implant-damaged layer. The procedure is different from that of Smart-Cut for silicon because of the much greater inertness and fragility of typical metal oxides.[10,11] This paper reports BTO single-crystal (100) thin-films obtained by ion slicing.

CIS utilizes the modification of the chemical and physical properties of materials by ion implantation to slice mesoscopically thin, single-crystal films.[6] Light ions are injected into a single-crystal bulk to form a sharp peak in the ion distribution at a depth determined by the energy of ions. The heavily implanted layer has different chemical and mechanical properties than the original single crystal. Thin films can be sliced from the bulk by wet etching or by thermal ramping of this sacrificial layer. The details of the slicing method depend on the specific material. For instance, lithium niobate slicing uses wet etching in hydrofluoric acid.[7]

In this letter, we show that large barium titanate films (see Fig. 1) can be obtained by thermal treatment of an implanted sample, which has been prebonded onto a glass wafer; a similar process has been applied to separating strontium titanate films.[9] Such thermally induced slicing by heating can be explained by the evolution of voids, which are created by implantation and spread by the high pressure of an interstitial implanted element. The Griffith theory for fracture growth shows that these voids spread until they are merged together, separating the thin top-layer from the bulk substrate when the size of a void becomes larger than a critical value.[12]

The BTO wafers used here are commercially available one-side-polished, (100)-oriented single crystal samples. Hydrogen implantation is done at H_2^+ ion energies of 0.26, 1.2, and 2 MeV. TRIM simulations show that the ion distribution peaks at depths of ~ 0.5, 4.7, and 8 μm, respectively. The charged hydrogen is injected into the BTO surface at an incident angle of 5° to avoid ion channeling. The wafer is cooled so as to maintain the BTO at $\sim 50\,^{\circ}$C during implantation, to avoid dynamic annealing of the sacrificial layer. Implantation increases the optical absorption of the crystal such that a dark green color is found after implantation in contrast to its original yellow color. Note, however, that the BTO recovers its original color after annealing at $\sim 300\,^{\circ}$C during bonding. We attribute the ion-induced change to color-center formation. Finally, after implantation, domain structures can be observed by optical microscopy, as will be discussed later.

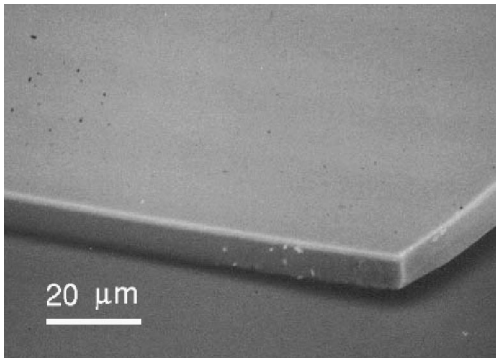

FIG. 1. A ~ 8-μm-thick BTO free-standing film.

[a]Electronic address: ti50@columbia.edu
[b]Also at Brookhaven National Laboratories, Upton, New York 11973.

The fragility of thin-films and the abrupt slicing process make it difficult to maintain the integrity of free-standing films during thermal slicing. Thus, a rigid handle wafer is often bonded onto the implanted target wafer for film support during processing. We used anodic bonding to attach the implanted BTO onto a glass handle wafer. The mechanism of anodic bonding is oxidation of the bond interface by the oxygen ions in the handle wafer of sodium borosilicate glass. A voltage is applied between the wafers, after the contacted BTO/glass wafer pair is heated to the activation temperature of mobile ions in the glass. Oxygen ions are injected into the bond interface so as to oxidize the contacted surface and fill the interfacial gap.[13] Because of the mobile ions within the glass and conductivity of the target wafer, current flows through the interface. The bonding process can be monitored by measurement of the anodic current. Finally, since the bonding temperature is higher than the BTO slicing temperature, the ion slicing step occurs *during* the formation of the bond.

The specific details of the procedure are as follows. An implanted BTO wafer is contacted to commercially available Pyrex™ glass(Corning code 7740) in air at room temperature. The sample pair is then heated slowly on a hot plate to 290–340 C under a voltage of 1400 V applied across the 1.5-mm-thick BTO/glass sample. Note that this temperature is much higher than the Curie temperature of BTO, that is, 120 °C. The bonding current, measured during the process, is consistent with the bonding mechanism discussed earlier; the onset of a current decrease indicates completion of bonding. The bond interface can be observed under an optical microscope through either of the transparent films. The absence of optical fringes showed that the bond between the BTO and the glass was intact across the entire sample surface. The bond was found to retain its integrity after immersion in water, acids, acetone, or methanol.

Atomic force microscopy (AFM) was used to investigate the surface topography after the ion slicing processes. Note that prior to implantation, the BTO wafers had a single domain structure and ~1 nm Ra roughness. Immediately after the implantation, BTO wafers show multidomain structure. Figure 2 shows AFM images of the surface following implantation and slicing. These images showed a periodic structure in the surface topography. Typically multidomain BTO has a 90° a,c-domain structure, in which adjacent domains have the c-axes perpendicular to each other.[1] The periodic band patterns on the BTO surface following implantation imply the formation of these same 90° domains. The identification of these features as domains was confirmed by measuring the surface structure of the pattern by AFM. Because of the tetragonal nature of BTO crystals at room temperature and the requirement for continuity and matching of the lattice, the angle between polar axes of adjacent domains differs slightly from 90°. By applying the condition for lattice matching between the two domains, this angle can be calculated to be $\Delta\theta = 90° - 2\arctan(a/c)$, where a and c are the lattice constants. The surface slope ($\Delta\theta$) of implanted and sliced BTO is measured to be $0.66 \pm 0.05°$, which agrees with the estimated value of 0.57° based on bulk BTO lattice constants.[14]

We conclude from the AFM observations that the domain structure following implantation is alternating a,c-domains, with the sliced films maintaining single-crystal lattice constants. This domain structure is most probably formed by the implanted-ion-induced mechanical stress introduced in the the implanted layer.[8] Figure 2 shows that the domain structure has a similar periodicity *after the slicing process*, even though the slicing is done at temperatures above the Curie point. This implies that the stress, which caused the multidomain formation, is not enhanced during slicing. Complete elimination of the stress may require a higher temperature annealing than the slicing temperature. Finally note that these domains can also be readily observed under an optical microscope with polarized light due to the birefringence and polarization orientation; only c-domains are optically isotropic.

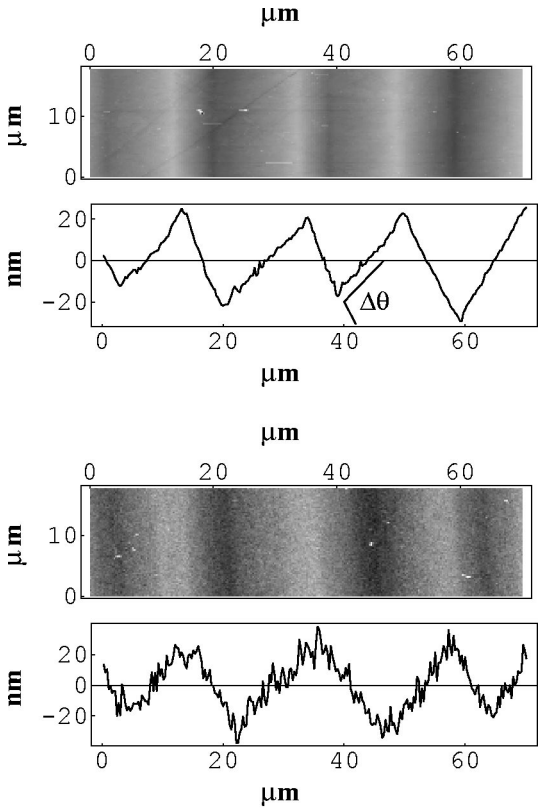

FIG. 2. AFM analysis of implanted(top) and sliced(bottom) BTO surface. The surface profile identifies the domain structure.

The measured roughness of the top surface after implantation is 1.1-nm Ra, excluding the effect of domain structure. This value is virtually equivalent to that of the original surface. However, the appearance of the domain structure introduces a regular surface structure of 9 nm. This structure does not effect the bonding process just discussed, which can bond to much rougher surfaces. Previous studies[6–9] have shown that a sliced surface can become somewhat rougher due to void formation within the sacrificial layer during the heating and slicing process (Fig. 2). In our case, the roughness of the slicing surface, excluding the regular domain structure, increased to only 5.6 nm. Finally, note that the largest change in surface topology during the entire slicing process is 90° domain formation; this structure can be removed by repoling of the multidomain structure into a single domain.

Measurements of the dielectric properties of the BTO

TABLE I. Dielectric properties of a bulk and film BTO measured by NSMM at room temperature.

	Permittivity (ϵ_c)	Loss tangent
Bulk BTO	264.7	0.263
Film BTO	240.4	0.095

film were done using a near-field scanning microwave microscope (NSMM).[15] In these measurements, microwave radiation at 1.7 GHz is coupled to the sample from a resonant structure via a near-field metallic tip, and any shifts in the resonant frequency and the quality factor are measured. The analysis, based on these shifts, gives the film permittivity and loss tangent.[16] The dielectric properties of the BTO films are extracted from the raw data by taking into account the glass substrate, to which the films are bonded. Table I shows the measured permittivity and loss for both film and bulk BTO. The measurement shows that the film retains the permittivity of the bulk crystal and has *lower* dielectric loss. We attribute this change in dielectric loss to stress induced by residual implanted ions[8] and by a thermal expansion mismatch between the substrate and the film. Stress is known to change the dielectric loss through interaction of the electromagnetic wave with lattice phonons.[17] The magnitude of change is consistent with previously reported values of changes in loss observed with an electric field.[18]

The permittivity of the sliced BTO films was measured using an integrated capacitor on the film surface. The patterned electrodes were fabricated on bonded ion-sliced BTO films. Specifically, interdigitated electrodes, 7 mm long and with a 20-μm-wide gap, were written by direct laser lithography followed by wet-etching of a metal layer deposited on the BTO surface. Note that the length of the electrodes is much longer than the domain width, so that multiple domains were sampled by the process. The capacitance between these electrodes was then measured at 100 MHz at room temperature with a network analyzer.

Using this process, we measured an in-plane capacitance on a 4.6-μm-thick BTO film of 23.3 pF. An effective permittivity of the film then could be calculated from the capacitance and the structure of the device to give an effective permittivity of $\sim$2300. This value is consistent with it being an average of the known ϵ_c and ϵ_a due to the multidomain structure.[19] This result also shows that the ϵ_a of the films, which is too large to be measured by our NSMM setup, is also single-crystal quality. Because of the bulk-like permittivity of CIS single-crystal thin films, the measured permittivity, $\sim$2300, is much larger than the reported value for high-quality epitaxial films with similar electrode structure, $\sim$400.[5] This large permittivity makes it possible to fabricate a small-sized, large-capacitance, integrated capacitor on CIS single-crystal films.

To summarize, barium titanate single-crystal thin-films have been obtained using ion slicing from bulk, single-crystal wafers. Anodic bonding to a glass support substrate allows large-area, $\sim$1-cm^2 films to be fabricated. The surface roughness and domain structure have been studied by AFM, and dielectric constant and loss in the films have been measured.

The authors wish to thank Prof. J. Yardley for his helpful comments during the course of this work. This project was supported by the FAME program under DARPA Grant No. N00173-98-1-G014 (T.I., I.G., and R.M.O.), N00173-98-G013 (Y.M.T. and M.E.R.) and RFLICS program under AFOSR Grant No. F30602-00-C-0128 (T.I., I.G., and R.M.O.).

[1] F. Jona and G. Shirane, *Ferroelectric Crystals* (Dover, New York, 1993).
[2] Y. S. Lee, B. K. Ju, D. H. Kim, and M. H. Oh, IEEE Trans. Electron Devices **48**, 653 (2001).
[3] S. E. Park, S. Wada, L. E. Cross, and T. R. Shrout, J. Appl. Phys. **86**, 2746 (1999).
[4] H. Y. Lee, T. C. Chen, and H. F. Yau, Appl. Opt. **39**, 6656 (2000).
[5] B. H. Hoerman, G. M. Ford, L. D. Kaufmann, and B. W. Wessels, Appl. Phys. Lett. **73**, 2248 (1998).
[6] M. Levy, R. M. Osgood, Jr., A. Kumar, and H. Bakhru, Appl. Phys. Lett. **71**, 2617 (1997).
[7] M. Levy, R. M. Osgood, Jr., R. Liu, L. E. Cross, G. S. Cargill III, A. Kumar, and H. Bakhru, Appl. Phys. Lett. **73**, 2293 (1998).
[8] M. Levy, R. M. Osgood, Jr., A. S. Bhalla, R. Guo, L. E. Cross, A. Kumar, S. Sankaran, and H. Bakhru, Appl. Phys. Lett. **77**, 2124 (2000).
[9] F. J. Kub, K. D. Hobart, J. M. Pond, and S. W. Kirchoefer, Electron. Lett. **35**, 477 (1999).
[10] M. Bruel, Electron. Lett. **31**, 1201 (1995).
[11] Q. Y. Tong, S. Gutjahr, S. Hopfe, U. Gösele, and T. H. Lee, Appl. Phys. Lett. **70**, 1390 (1997).
[12] C. M. Varma, Appl. Phys. Lett. **71**, 3519 (1997).
[13] K. B. Albaugh and D. H. Rasmussen, J. Am. Ceram. Soc. **75**, 2644 (1992).
[14] S. Tsunekawa, T. Fukuda, T. Ozaki, Y. Yoneda, T. Okabe, and H. Terauchi, J. Appl. Phys. **84**, 999 (1998).
[15] Y. G. Wang, M. E. Reeves, W. J. Kim, J. S. Horwitz, and F. J. Rachford, Appl. Phys. Lett. **78**, 3872 (2001).
[16] Y. M. Tesfu and M. E. Reeves (unpublished).
[17] V. L. Gurevich and A. K. Tagantsev, Adv. Phys. **40**, 719 (1991).
[18] Y. M. Poplavko, Sov. Phys. Solid State **6**, 45 (1964).
[19] G. W. Farnell, I. A. Cermak, P. Silvester, and S. K. Wong, IEEE Trans. Sonics Ultrason. **SU-17:188** (1970).